Threshold Laser Intensity Refinement and Scenarios for Observation of QED Cascade Production

Alexander Fedotov, Nikolay Narozhny and Arseny Mironov

National Research Nuclear University MEPhI (Moscow Engineering Physics Institute), Kashirskoe sh. 31, 115409 Moscow, Russian Federation

E-mail: `am_fedotov@mail.ru`

Abstract. Previously we have proposed simple qualitative estimates for threshold laser intensity required to observe the laser-induced self-sustained QED (or A-type) cascades. They were later brilliantly confirmed by simulation of cascades arising in a rotating purely electric field. However, in view of numerous simulations performed since then for a more realistic setup our previous criterium of arising of self-sustained cascades may now seem to be too conservative thus essentially overestimating the intensity actually required. After refining our estimates and explaining the origin of assumptions and discrepancies with some new simulation results, we present and discuss in details two particular experimental schemes for their observation. These schemes in different ways overcome a non-trivial problem of injection of seed particles into the focal region and are optimized to lower the threshold intensity value as much as possible.

1. Introduction
Recently, significant attention was payed [1–13] to predictions [14, 15] of emergence of self-sustained electron-positron-photon (QED) cascades in interaction of high-intensity laser fields with matter. The self-sustained (or A-type) cascades in laser field should be distinguished from the ordinary (or S-type) cascades, see Table 1, as they typically grow up exponentially, thus probably dominating in laser plasma dynamics at high intensities. As of now, both the threshold and saturation mechanisms of A-type cascades in the context of laser-matter interactions are still under discussion.

2. Threshold laser intensity refinement
The original estimates [15] for a threshold intensity of A-type cascade generation were based on few assumptions. First, for $E \ll E_S = m^2 c^3 / e\hbar = 1.3 \cdot 10^{16}$V/cm ($I \ll 10^{29}$W/cm^2) electron motion between the events of hard photon emission can be treated classically. Second, assuming $a_0 \gg 1$, on the one hand, the formation time of the processes of hard photon emission and pair photoproduction $t_{form} \simeq mc/eE \ll 1/\omega$, hence one can use the locally constant field approximation. On the other hand, particles are ultrarelativistic ($\gamma \sim a_0 \gg 1$) and the field in their reference frame looks as crossed field ($E \approx B$, $\vec{E} \perp \vec{B}$). Under such conditions, the probability rates of hard photon emission and pair photoproduction processes are controlled by a single parameter,

$$\chi = \frac{e\hbar}{m^3 c^4} \sqrt{-(F_{\mu\nu} p^\nu)^2} \simeq \frac{\gamma \left| \left(\vec{E} + \frac{\vec{v}}{c} \times \vec{B} \right)_\perp \right|}{E_S}, \tag{1}$$

Table 1. Characterization of S(shower)- and A(avalanche)-type cascades

S(shower)-type	A(avalanche)-type
produced by energy ε_0 of seed particle	field donates energy by reaccelerating secondary particles
proceeds until particles loose their energy ($N_{e^+e^-}^{(max)} \propto \varepsilon_0$)	multiplicity is growing exponentially ($N_{e^+e^-}(t) \propto e^{\Gamma t}$) until: • field depletion [3], or • particles escape, or • thermolization of e^+e^- plasma • ... (?)
similar to Extensive Air Showers	similar to gas or dielectric breakdown
almost observed in E144 SLAC experiment	never observed in laboratory

which we call the dynamical quantum parameter. For $\chi \gtrsim 1$ these rates are given by

$$W_\gamma(\chi_e \gtrsim 1) \simeq 1.64 \frac{\alpha m^2 c^4}{\hbar \varepsilon_e} \chi_e^{2/3}, \quad W_{e^+e^-}(\chi_\gamma \gtrsim 1) \simeq 0.23 \frac{\alpha m^2 c^4}{\hbar \varepsilon_\gamma} \chi_\gamma^{2/3}, \tag{2}$$

but for $\chi_\gamma \ll 1$ pair photoproduction process is exponentially supressed $[W_{e^+e^-} \simeq \mathcal{O}(e^{-8/3\chi_\gamma})]$.

Analysis of classical equation of motion $\dot{\vec{p}} = \vec{F}_L$ shows that if the particle is initially at rest and the field direction is time-varied, then the angle ϑ between the particle momentum $\vec{p}$ and the Lorentz force $\vec{F}_L$ is typically growing initially, $\vartheta(t) \simeq \omega t$. This conjecture was proved for a model of uniformly rotating electric field [1] and the general proof is sketched in [16]. This means that the particle energy and the dynamical quantum parameter are initially growing as

$$\varepsilon(t) \simeq eEct, \quad \chi(t) \simeq \frac{E_\perp}{E_S}\gamma \sim \frac{E\vartheta}{E_S}\gamma \simeq \frac{E\omega t}{E_S} \cdot \frac{eEt}{mc} \sim \left(\frac{E}{E_S}\right)^2 \frac{\omega}{\hbar/mc^2} t^2. \tag{3}$$

The latter approaches unity $[\chi(t_{acc}) \sim 1]$ during the time interval

$$t_{acc} \simeq \frac{1}{\omega} \cdot \frac{\alpha E_S}{E} \cdot \sqrt{\frac{\hbar\omega}{\alpha^2 mc^2}} \simeq \frac{1}{\omega} \cdot \frac{\alpha E_S}{E}, \tag{4}$$

where, for simplicity, we have used the fact that for optical lasers ($\hbar\omega \sim 1\text{eV}$) the square root is accidentally of the order of unity[1]. In what follows, we call (4) the acceleration time.

Since the rates (2) differ only by numerical factor, the free path time t_{free} of electrons, positrons and hard photons with respect to the processes of hard photon emission and pair photoproduction, respectively, can be derived by equating $\frac{1}{t_{free}} \sim W(t_{free}) \sim \frac{\alpha m^2 c^4}{\hbar \varepsilon(t_{free})}\chi^{2/3}(t_{free})$, where $\varepsilon(t)$ and $\chi(t)$ are given by (3). In this way we obtain

$$t_{free} \simeq \frac{1}{\omega}\left(\frac{\alpha E_S}{E}\right)^{1/4}\sqrt{\frac{\hbar\omega}{\alpha^2 mc^2}} \simeq \frac{1}{\omega}\left(\frac{\alpha E_S}{E}\right)^{1/4}. \tag{5}$$

---

[1] In fact, $Ry = \alpha^2 mc^2$ is nothing but the typical atomic energy scale for a hydrogen (Rydberg).

Since all the particles are ulrarelativistic on average, the time of their escape from the focus in case of extremely tight focusing ($w_0 \sim 1/\omega$) can be estimated as

$$t_{esc} \simeq \frac{1}{\omega}. \tag{6}$$

Hence, by comparing Eqs. (4), (5) and (6) we conclude that the condition

$$E \gtrsim \alpha E_S \quad (\text{or} \quad a_0 \gtrsim 3700, \quad I \gtrsim 5 \cdot 10^{25} \text{W/cm}^2), \tag{7}$$

should define the threshold intensity for the onset of cascade production. Indeed, under the condition (7) two inequalities

$$t_{acc} \lesssim t_{free} \lesssim t_{esc}$$

are respected simultaneously. The first one ensures that namely hard photons, which are capable for further pair production, are mainly emitted. The second one guarantees that the number of generations of secondary particles arising from each of the seed particles, is larger than unity ($N_{e^+ e^-} \simeq e^{t_{esc}/t_{free}} \gtrsim 1$), i.e. that the process is a cascade in nature. Under these condition the average quantities characterizing the population of secondary particles, are given by

$$\frac{\Gamma}{\omega} \simeq \left(\frac{E}{\alpha E_S}\right)^{1/4} \gg 1, \quad \chi \simeq \left(\frac{E}{\alpha E_S}\right)^{3/2} \gg 1, \quad \varepsilon \simeq \frac{mc^2}{\alpha}\left(\frac{E}{\alpha E_S}\right)^{3/4}, \quad \vartheta \simeq \left(\frac{\alpha E_S}{E}\right)^{1/4} \ll 1. \tag{8}$$

The scalings (8) were brilliantly approved by simulations in a uniformly rotating electric field model [1]. However, most of later simulations adopting more realistic setup reported observation of cascade production at somewhat lower intensity level ($10^{23 \div 24}$W/cm^2, i.e. $1 \div 2$ orders of magnitude lower than our prediction (7)). We emphasize that determination and understanding of an actual intensity threshold value for A-type cascade production is of ultimate importance for such projects as ELI or XCELS.

Here, let us point out several possible reasons that could explain why the criterium (7) may in fact overestimate the actual threshold (as observed in realistic simulations):

(i) First of all, according to practice, different independently designed codes typically show (at least, slightly) different results. This may originate in either different account for soft part of electron radiation, or implementation of different event generators, or other issues (including possible bugs). Hence, we call the community to work out together some minimal set of tests to benchmark the codes;

(ii) An obvious origin of possible discrepancy comes from using the naive assumption (6) about the time of residence of particles in the strong field region. First, in most realistic simulations presented by now focusing was not as tight (typically, $w_0 \simeq 3 \div 10\lambda$). Second, the escape time may be essentially larger because of complicated motion of electrons in a standing-wave field, as well as due to possible radiation trapping effect [17]. Obviously, increasing of t_{esc} due to any reason would be always favorable for cascade production.

(iii) Finally, let us note that any estimate of average Γ would unavoidably overestimate the threshold due to purely statistical reasons. First, we always have $\langle N \rangle \simeq \langle e^{\Gamma t} \rangle \geq e^{\langle \Gamma \rangle t}$ and moreover, this inequality becomes stronger the larger is computation time t. Secondly, the threshold value of photon dynamical parameter triggering pair photoproduction is not sharp but fuzzy. We essentially assumed in estimation that pairs can be only created when $\chi_\gamma \gtrsim 1$, however in simulations it was observed that photons with even $\chi_\gamma \simeq 0.1$ were capable for pair creation.

We think that these observations and refinements could explain an apparent contradiction between our early estimates [15] and some recent simulations.

3. Possible experimental scenarios

We assumed above that the initial seed particle is already located somewhere near the center of the focal region. However, it turns out that in real life injection of seed particles into the strong field region is by no means a trivial task. In a typical setup the field is turned on gradually. Under such conditions the electrons of the target usually have well enough time to be expelled by ponderomotive force from the region where the field is increasing long before it achieves its peak values [18].

On the other hand, injection of seed charged particles (electrons) into the focus from outside may be prevented by radiation reaction (Pomeranchuk theorem, [19]). Indeed, assuming a high-energy particle is approaching the strong field region so that radiation reaction force dominates over the Lorentz force in the Landau-Lifshitz equation, we have

$$m\frac{d\gamma}{dt} \approx -\frac{2}{3}\frac{e^4}{m^2}\underbrace{\left[(\vec{E}+\vec{v}\times\vec{H})^2 - (\vec{v}\cdot\vec{E})^2\right]\Big|_{\vec{r}=\vec{\rho}+\vec{v}t}}_{F_\perp^2(t)}\gamma^2,$$

so that

$$-\int_{\gamma_i}^{\gamma_f}\frac{d\gamma}{\gamma^2} = \frac{1}{\gamma_f} - \frac{1}{\gamma_i} = \frac{2}{3}\frac{e^4}{m^3}\int_{t_i}^{t_f}F_\perp^2(t)\,dt,$$

hence

$$\gamma_f^{(max)} = \frac{3}{2}\frac{m^3}{\alpha^2\int\limits_{-\infty}^{0}F_\perp^2(t)\,dt} \sim \frac{3}{2}\frac{m^3}{e^4\frac{1}{2}\left(\frac{m\omega a_0}{e}\right)^2 R} = \frac{3m}{e^2 a_0^2 \omega^2 R},$$

meaning that its γ-factor in the strong field region is bounded exclusively by the parameters of the field (namely, the field strength and typical size R of the strong field region) independently on its initial energy. Such a particle will never be able to overcome ponderomotive repulsion of the strong field region if

$$\gamma_f^{(max)} \lesssim a_0, \quad \text{or} \quad a_0 \gtrsim \left(\frac{3m}{e^2\omega^2 R}\right)^{1/3}. \tag{9}$$

This conclusion was confirmed by numerical simulations [17, 20] and remains qualitatively true when radiation reaction is treated as quantum (even though Pomeranchuk theorem is no more valid literally in such a case).

3.1. Seed particles injection scenario

Still, hard γ-quanta emitted by such high-energy particles approaching the focus can penetrate inside and initiate cascades. In our initial estimations, we assumed that A-type cascade is seeded by a charged particle, which is initially slow or at rest in the strong field region. In the scenario now under consideration, secondary hard γ-quanta approaching the strong field region typically initiate an S-type cascade. However, if the field is strong enough to support development of A-type cascades (whatever the actual threshold value is) and, in addition, the depletion time of the S-cascade

$$t_S \simeq t_{free}\cdot n \simeq \frac{\hbar\varepsilon_i}{\alpha m^2 c^4}\chi_i^{-2/3}\cdot\log_2\left(\frac{\chi_i}{\chi_{min}}\right)$$

(where n is the number of generations and $\chi_{min} \simeq 0.1$ is the effective threshold for pair photoproduction, see above) is tuned so that the S-type cascade decays due to energy losses exactly when the secondary particles are about to approach the focal region,
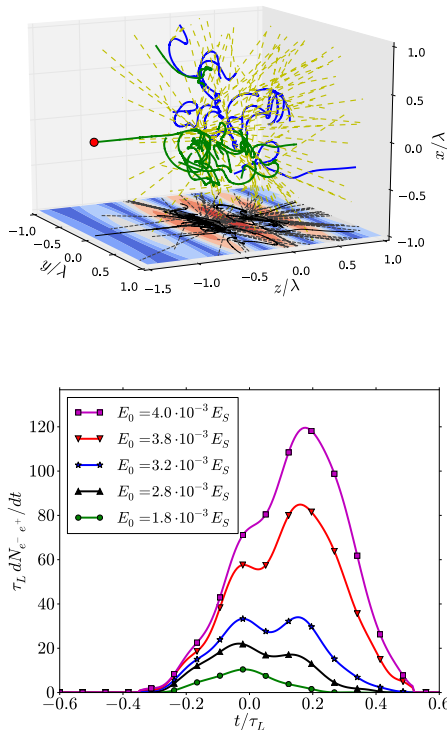
$$t_S \sim \tau_L/2, \tag{10}$$

Figure 1. Visual tracks of electrons (green), positrons (blue) and hard photons (dashed dark yellow) in the cascade (seed electron is marked by a red circle) initiated by 3Gev electron in the field of two counterpropagating circularly polarized laser pulses. of strength $E_0 = 3.2 \cdot 10^{-2} E_S$ ($a_0 = 1600$, $I \simeq 5 \cdot 10^{24} \mathrm{W/cm^2}$). On bottom, distribution of electric field is shown.
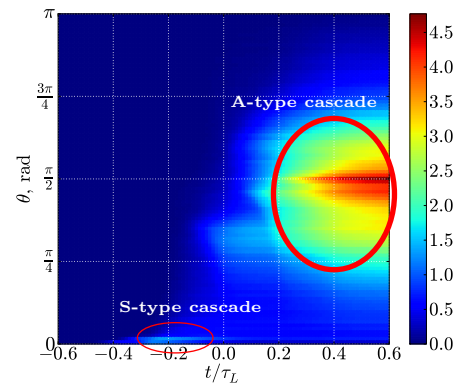

Figure 2. Positron production rate for a setup with two counterpropagating circularly polarized 10fs laser pulses. Cascades are seeded by a 3GeV copropagating electron beam (as in Fig. 1) [21].

Figure 3. Typical time scanned angular distribution of hard γ-quanta in simulation (parameters are the same as in Fig. 2).

then these secondary particles penetrating the focal region can later trigger an A-type cascade as well [21].

Simulation results for such a setup are demonstrated in Figs. 1–3. Emergence of both (S- and later A-) types of cascades can be observed from either the distinctive two-hump profile of time dependence of the pair creation rate (Fig. 2), or from time scanned angular distribution of emitted hard photons (Fig. 3), the latter as they are all emitted only in forward direction, and as A-type cascade is formed by relatively slow particles, accelerating and radiating mostly in perpendicular plane. As the field is increased, the second (right) peak in Fig. 2, corresponding to an A-type cascde, is growing. Interestingly, the outgoing secondary particles of the arising A-type cascade are propagating almost along the nodes of the electric field (Fig. 1).

3.2. Multibeam scenario
An alternative scenario is to compress the seed by multiple coherent colliding beams, preventing it from fast escape outwards. The idea is similar to the one already used to enhance spontaneous pair production in [22]. As in [22], the additional benefit of such setup arises because the field strength at focal center is essentially increased due to constructive interference. However, unlike [22], here we start from differently elliptically polarized individual beams and search for their optimal polarizations. Intuitively, the beams should be focused as tightly as possible (this
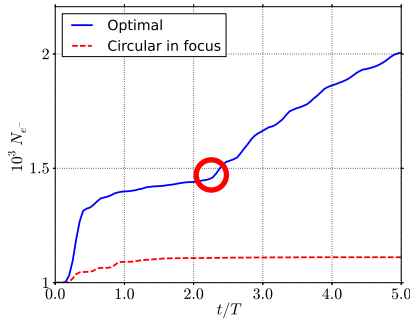
Figure 4. Number of electrons in a cascade vs time (in laser periods) for optimal (blue solid) and circular (red dashed) polarization of the total field (8 beam plane setup, $P = 7.9$PW, adopted from [16]).

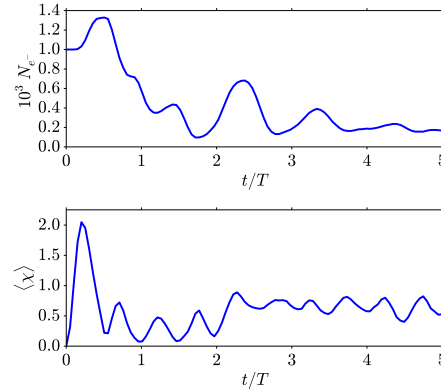**Figure 5.** Number of electrons located at a distance smaller than wavelength from the origin (top) and their mean value of parameter χ (bottom). [16].

should also minimize their required number, which is obviously also preferable experimentally). In case of focusing aperture 0.2π (which is today's state-of-the-art) the number of colliding beams is limited by avoidance of mutual peripheral intersections to 8 in plane geometry and to 16 in a spatial one.

Optimization with respect to polarizations of individual beams, targeting at minimizing t_{acc} as much as possible, reveals the non-trivial results [16]. In the optimal case all the beams should be polarized individually in such a way that the total field is polarized elliptically, with $\sqrt{2} : 1$ axes ratio. This result was tested by Monte Carlo simulations based on a particular 3D model of Gaussian beams. Growth of the number of pairs in a 8-beam plane setup is compared for the optimal and circular polarizations of the beams of the same net power in Fig. 4. It is evident that optimal polarization is indeed superior. An interesting feature is a bend (marked by a red circle) of the optimal curve at $t \approx 2.2T$. At exactly the same moment the mean value of the parameter χ of those particles which are near the focus turns up, see Fig. 5. This shows that particle dynamics is complicated and is yet far from clear. The threshold power and intensity found in this way are $P_{th} \simeq 7.9$PW ($I_{th} \simeq 5.6 \cdot 10^{23}$W/cm^2) for the (optimal) 8-beam plane setup and $P_{th} \simeq 6$PW ($I_{th} \simeq 4 \cdot 10^{23}$W/cm^2) for 16-beam spatial setup. Because several assumptions were made prior to optimization, it would be probably possible to decrease these threshold values even further.

4. Conclusion

Two types (S- vs. A-) of QED cascades in laser filed should be distinguished. Qualitative theory [15] predicted threshold laser intensity level $\simeq 5 \cdot 10^{25}$W/cm^2 for A-type cascades generation. This theory was reviewed and several reasons for simulations-based refinement of the threshold have been discussed. In spite of 'radiative impenetrability' of the strong field region (laser focus), A-type cascades can be still seeded by secondary hard photons, demonstrating cascade 'collapse and revival' effect at $I \simeq 5 \cdot 10^{24}$W/cm^2. With a more sophisticated (coherent) multibeam setup it is even possible to initiate cascades at the intensity level $5 \cdot 10^{23}$W/cm^2.

References
[1] Elkina N, Fedotov A, Kostyukov I Y, Legkov M, Narozhny N, Nerush E and Ruhl H 2011 *Phys. Rev. ST Accel. Beams* **14** 054401
[2] Kirk J G, Bell A and Arka I 2009 *Plasma Phys. Contr. Fusion* **51** 085008
[3] Nerush E, Kostyukov I Y, Fedotov A, Narozhny N, Elkina N and Ruhl H 2011 *Phys. Rev. Lett.* **106** 035001
[4] Duclous R, Kirk J G and Bell A 2011 *Plasma Phys. Contr. Fusion* **53** 015009
[5] Ridgers C, Brady C S, Duclous R, Kirk J, Bennett K, Arber T, Robinson A and Bell A 2012 *Phys. Rev. Lett.* **108** 165006
[6] Kirk J, Bell A and Ridgers C 2013 *Plasma Phys. Contr. Fusion* **55** 095016
[7] Lobet M, d'Humières E, Grech M, Ruyer C, Davoine X and Gremillet L 2013 *arXiv:1311.1107*
[8] Bashmakov V, Nerush E, Kostyukov I Y, Fedotov A and Narozhny N 2014 *Phys. Plasmas* **21** 013105
[9] Brady C, Ridgers C, Arber T and Bell A 2014 *Phys. Plasmas* **21** 033108
[10] Gonoskov A, Bastrakov S, Efimenko E, Ilderton A, Marklund M, Meyerov I, Muraviev A, Sergeev A, Surmin I and Wallin E 2015 *Phys. Rev. E* **92** 023305
[11] Jirka M, Klimo O, Bulanov S, Esirkepov T Z, Gelfer E, Bulanov S, Weber S and Korn G 2015 *arXiv:1511.04982*
[12] Grismayer T, Vranic M, Martins J L, Fonseca R and Silva L O 2015 *arXiv:1511.07503*
[13] Chang H, Qiao B, Xu Z, Xu X, Zhou C, Yan X, Wu S, Borghesi M, Zepf M and He X 2015 *Phys. Rev. E* **92** 053107
[14] Bell A and Kirk J G 2008 *Phys. Rev. Lett.* **101** 200403
[15] Fedotov A, Narozhny N, Mourou G and Korn G 2010 *Phys. Rev. Lett.* **105** 080402
[16] Gelfer E G, Mironov A A, Fedotov A M, Bashmakov V F, Nerush E N, Kostyukov I Y and Narozhny N B 2015 *Phys. Rev. A* **92**(2) 022113
[17] Fedotov A, Elkina N, Gelfer E, Narozhny N and Ruhl H 2014 *arXiv:1408.0362*
[18] Tamburini M, Di Piazza A and Keitel C H 2015 *arXiv:1511.03987*
[19] Pomeranchuk I Y 1940 *J. Phys. USSR* **2** 65
[20] Elkina N, Fedotov A, Herzing C and Ruhl H 2014 *Phys. Rev. E* **89** 053315
[21] Mironov A, Narozhny N and Fedotov A 2014 *Phys. Lett. A* **378** 3254–3257
[22] Bulanov S, Mur V, Narozhny N, Nees J and Popov V 2010 *Phys. Rev. Lett.* **104** 220404